

Rare earth element geochemistry of the Permo-Carboniferous clastic sedimentary rocks from the Spiti Region, Tethys Himalaya: significance of Eu and Ce anomalies

Javid Ahmad Ganai · Shaik Abdul Rashid

Received: 16 January 2014 / Revised: 21 February 2014 / Accepted: 24 February 2014 / Published online: 17 February 2015
© Science Press, Institute of Geochemistry, CAS and Springer-Verlag Berlin Heidelberg 2015

Abstract Siliciclastic sedimentary rocks, including sandstones and associated shales, from the Permo-Carboniferous Kanawar Group of NW Tethys Himalaya, Spiti Region, India were examined geochemically to monitor the evolutionary changes in the upper continental crust in the Himalaya. The rocks are characterized by consistent rare earth element (REE) patterns with light REE enrichment ($\text{La}_N/\text{Yb}_N = 5.3\text{--}28.2$) and flat heavy REE patterns. The $\sum\text{REE}$ values are high (up to 281 ppm) with large negative Eu anomalies (avg. $\text{Eu}/\text{Eu}^* = 0.57$). The REE characteristics of the sediments are similar to those of post-Archean Australian shales and North American shale composite. La/Th values (avg. 2.34) correspond to a relatively felsic composition of the terrestrial igneous rocks standard (La/Th of G-1 = 2.3). The evolved felsic composition of the sediments probably relates to widespread acidic activity in the source. The REE patterns and Th/U values seem to have been affected by the sedimentary environment as well as by the provenance. The presence of positive Ce anomalies in some sediments may be the result of post-depositional processes. Moreover, the Permo-Carboniferous sediments indicate that hydraulic sorting, even over short transport distances, is capable of concentrating enough accessory phases to influence REE composition and to develop negative Eu anomalies. High $\sum\text{REE}$, La/Yb , and Th/U contents and large negative Eu anomalies reveal that the sediments were deposited in an oxidizing environment, suggesting the surficial environment became oxidizing around the Carboniferous-Permian boundary in the Indian craton.

Keywords Late Paleozoic sediments · Tethys Himalaya · REE geochemistry · Provenance · Paleoclimate · Ce anomalies

1 Introduction

The geochemistry of terrigenous clastic sediments provides information about changes in the composition of the continental crust through time. For the last three decades several studies have been carried out to characterize the composition of the continental crust (Taylor and McLennan 1985, 1995; McLennan et al. 1993, 2001; Condie 1993; Barth et al. 2000; Yan et al. 2002; Rashid 2005; Garzanti et al. 2010; Moosavirad et al. 2011). The examination of trace element abundances in sedimentary rocks has added greatly to our understanding of crustal evolution, with rare earth element (REE) patterns and Th being particularly useful. These elements are transferred almost directly into clastic sedimentary rocks (McLennan et al. 1993). It has also been observed that these elements' distribution is uniform in fine-grained clastic sedimentary rocks and that they are resistant to weathering, diagenesis, and metamorphism (Cullers 1994; McLennan et al. 1993; Cullers 2000). Moreover, the residence times of REEs in seawater are short—50–600 years (McLennan et al. 1993, Garzanti et al. 2010)—and their concentration in the ocean is exceedingly low, being in the parts per trillion range.

Significantly, fundamental differences in the geochemistry (particularly trace elements, including REEs) of typical Archean and post-Archean sedimentary rocks reflect differences in the composition of the upper crust exposed to weathering (Taylor and McLennan 1985). An important discovery in this regard is that the REE patterns of post-Archean sedimentary rocks have shown remarkable

J. A. Ganai (✉) · S. A. Rashid
Department of Geology, Aligarh Muslim University,
Aligarh 202002, India
e-mail: jganai.ganai9@gmail.com

consistency (Taylor and McLennan 1985; Garzanti et al. 2011), and are generally characterized by a significant negative Eu anomaly. In contrast, Archean rocks generally have lower total REE abundances, less fractionated patterns (i.e., lower La/Yb), and almost invariably lack any significant negative Eu anomaly (McLennan et al. 1993). Condie, (1993) in a review of chemical composition and evolution of the upper continental crust (UCC), argues that a negative Eu anomaly characterizes both Archean and post-Archean rocks. However, he noticed that the size of the Eu anomaly is certainly greater in post-Archean UCC, a feature that is related to the Eu anomalies in rocks of felsic igneous provenance (Boryta and Condie 1990; Condie et al. 2001). It has also been argued that the change in composition of UCC is essentially related to the widespread intrusion of K-rich granitoids into the upper crust at the end of the Archean (Wronkiewicz and Condie 1990; McLennan and Taylor 1991; Condie et al. 2001). Changing REE patterns seen in some early Proterozoic successions represent the gradual unroofing of this added material. A decrease in the portion of mafics (Komatiites) and the massive acidic igneous activity marks the end of the Archean and thus defines the Archean-Proterozoic boundary at 2.7–2.5 Ga (McLennan et al. 1993; Condie 1993). These studies have clearly indicated that the composition of the exposed Archean crust was more mafic in

nature (less enriched in incompatible elements, with small negative Eu anomalies). Besides REEs, a number of other differences exist between Archean and post-Archean sedimentary compositions. Significant differences in major element composition have been recorded and are consistent with the more felsic upper crust in the post-Archean (McLennan 2001). The ferro-magnesium trace elements Cr and Ni are depleted while other incompatible elements (e.g., Th, U) are much higher in post-Archean sedimentary rocks.

In this paper we examine the REE geochemistry of Permo-Carboniferous sediments from the Kanawar Group, Spiti Region, NW Tethys Himalaya in the context of provenance, weathering effects, and evolutionary changes in UCC in the Himalaya. Since the sedimentary rocks under discussion are from a marine environment, the effects of environmental conditions on red-ox sensitive elements, particularly Eu and Ce, are also discussed.

2 Geological setting

The sedimentary succession of the Tethys Himalaya represents the deformed remnants of the northern continental margin of the Indian subcontinent. The succession, one of the most complete and spectacularly exposed in the world,

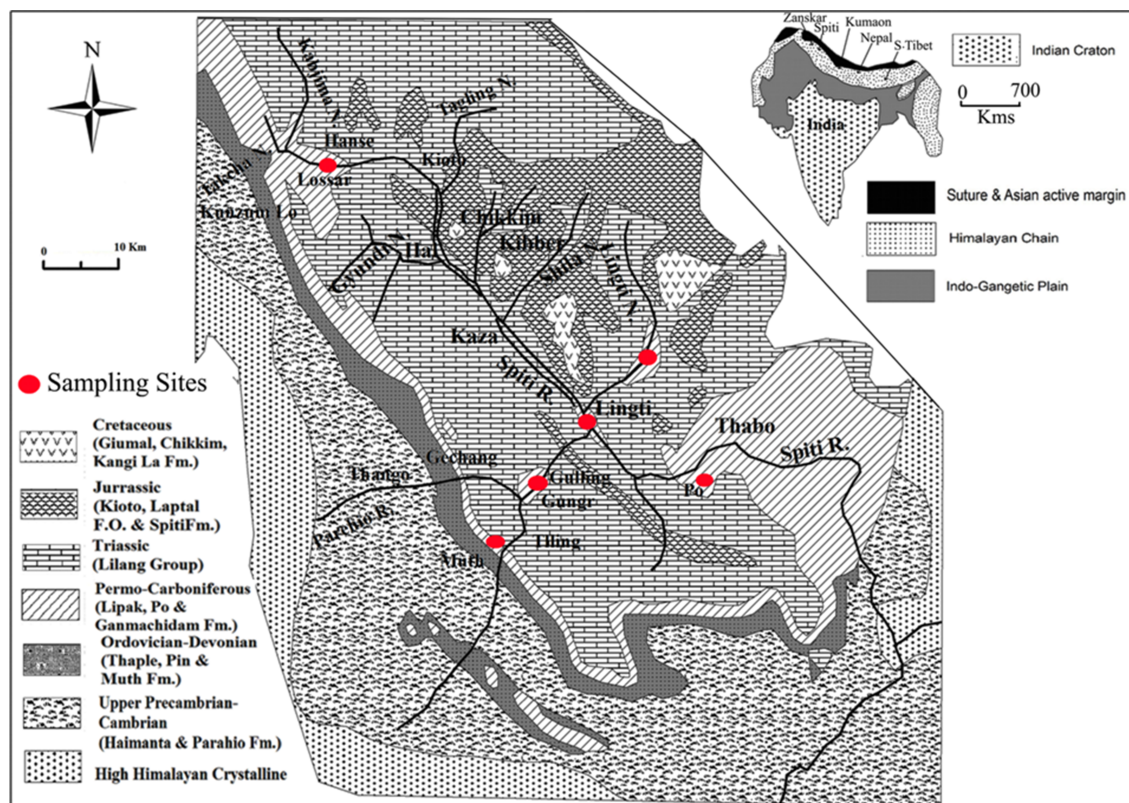


Fig. 1 Geological map of the Spiti Valley (after Bagati 1990)

preserves an excellent stratigraphic record of the Precambrian to Cretaceous period. Although involved in the tertiary Himalayan orogeny, the sedimentary succession experienced little deformation (low-grade metamorphism) and thus preserves the complete record of source rock compositions. The Spiti Region, containing an almost uninterrupted Phanerozoic succession of Tethyan Himalaya, is surrounded by Ladakh and Tibet in the north and north-east and the Higher Himalaya in the south (Fig. 1). The presence of a richly fossiliferous and fairly complete classical Phanerozoic sequence has attracted the attention of geoscientists around the globe. Detailed investigations by Bagati (1990), Gaetani and Garzanti (1991), Garzanti et al. (1996), Bhargava and Bassi (1998), Draganits et al. (2002), Myrow et al. (2003), Bhargava (2008), and Sciunnach and Garzanti (2012) have established various stratigraphic units of the Phanerozoic

sequence with remarkable precision mainly based on fossil assemblages. Based on extensive investigations by various geoscientists, a broad consensus has been reached to divide the Permo-Carboniferous sequence into two major groups (Table 1) although different opinions exist on subdivisions of these groups into formations and members. The present work is mainly confined to Late Paleozoic (Permo-Carboniferous) terrigenous rocks of the Tethyan sequence of the Spiti area, which includes the Lipak, Po, and Ganmachidam formations of the Kanawar Group (Table 1). These formations consist of clastic sediments—mostly shales, sandstones, and quartzites. The Permo-Carboniferous sections were investigated in detail in different localities exposed along the Spiti Valley from the Takche-Lossar, Muth-Kuling, Kabzima Nalla, and Lingti-Tabbo sections (Fig. 1) and over 40 samples were collected for geochemical analysis.

Table 1 Lithostratigraphic description of Permo-Carboniferous sequences of the Tethys Himalaya, Spiti region (after Bhargava 2008)

Group	Formation	Age	Lithology
	Mikin	Early-Triassic	Limestone
Disconformity			
K			
U			
L (Permian)	Gungri	Late-Permian	Gray to Dark gray needle, splintery blackshale with nodules and sandstones
I			
N	Gechang	Early-Permian	Calcareous sandstones and quartzites
G			
Disconformity			
K			
A			
N	Ganmachidam	Late-Carb.to Early Permian	Diamictites & quartzitic sandstones
A	Po	Upper early Carb. To Late Carboniferous	Black shales and quartzitic sandstones
W(Carboniferous)	Lipak	Early Carboniferous	Limestones with nodules and gypsum lenses, Dolomite, Shales, quartzitic sandstones
A			
R	Muth	Late Devonian	Quartzites

3 Analytical techniques

Representative samples were air-dried, coarsely crushed with a steel jaw crusher, and powdered in an agate mill down to a grain size smaller than 200 mesh. A total of 29 samples of siliciclastic sedimentary rocks were selected for analysis. Trace elements, including REEs and high field strength elements, were analyzed using inductively coupled plasma mass spectrometry (ICP-MS) at the National Geophysical Research Institute (NGRI), Hyderabad, India (Table 2). Analytical precision for trace elements is well within 5 %–10 %. The rock solutions were prepared using the technique given by Balaram and Gnaneshwar Rao (2003).

4 Discussion

4.1 REE characteristics in Tethys sediments

The REE patterns of the analyzed samples under discussion are shown in Fig. 2. Most of the sediments display patterns similar to typical post-Archean sediments such as the North American shale composite (NASC), post-Archean Australian shales (PAAS) etc., with light REE (LREE) enrichment [$(\text{La/Yb})_N = 5.34\text{--}28.22$, avg. = 13.53] and fairly flat heavy REE (HREE) patterns. Total REE abundances are variable ($\sum \text{REEs} = 171\text{--}281$ in shales; 39–212 in sandstones), which may be related to differing amounts of accessory minerals. The relatively low total abundances seen in some of the siliciclastic sedimentary rocks are probably due to dilution by quartz ($\text{SiO}_2 > 75\%$). Most significant are the prominent negative Eu anomalies (avg. $\text{Eu/Eu}^* = 0.58$) which are typical of post-Archean sediments ($\text{Eu/Eu}^* = 0.65$; McLennan et al. 1993). The HREEs show more uniform fractionation patterns [$(\text{Gd/Yb})_N = 1.18\text{--}4.22$; avg. 2.22] than the LREEs [$(\text{La/Sm})_N = 2.45\text{--}6.08$; avg. 3.78]. Both positive and negative Ce anomalies are found in these sediments. Fluctuations in the Ce anomaly may provide information regarding transgressive-regressive phases in terrestrially-derived near-shore marine sediments. During a regressive phase, eroded nearshore sediments may be enriched in Ce(OH)_4 thus increasing the positive Ce anomaly in marine sediments, whereas during a transgressive phase, there will be less deposition of Ce(OH)_4 -enriched sediments transported into deeper waters, resulting in a relative negative anomaly (Liu et al. 1988).

Apart from REEs, other elements were analyzed for comparison with post-Archean crust. McLennan (2001) examined Th and U data in sedimentary rocks as a function of age. Since the U is relatively mobile, the U data are not relevant. However, like REE, Th being insoluble during weathering and sedimentation because of very short residence time in seawater is meaningful. McLennan and

Taylor (1980) made an attempt to see the relation between La and Th in sedimentary rocks through time. They found a conspicuous compositional relationship for La/Th and Th/Yb: La/Th values increase and Th/Yb values decrease toward more mafic compositions. In other words, Archean crustal rocks, being relatively mafic in composition, should show an increase in La/Th and decrease in Th/Yb ratios relative to post-Archean sediments. This observation has been confirmed by McLennan et al. (1990) by analyzing clastic sedimentary rocks of widely varying age. Our results from the Spiti Region are consistent with studies carried out elsewhere. The correlation between La and Th in the sedimentary rocks is shown in Fig. 3. All our samples have a La/Th ratio between 2 and 4. Average La/Th and Th/Yb values determined for the Tethys Himalayan black shales are 2.34 and 8, respectively, which corresponds to a relatively felsic composition (La/Th and Th/Yb values of United States Geological Survey igneous rock standard G-2 are 2.3 and 27, respectively, data from table of McLennan et al. 1980).

4.2 Paleoweathering conditions of source rocks

Several intensive studies have been carried out to understand the chemical processes of weathering (Nesbitt et al. 1980) and their effects on the chemical composition of clastic sedimentary rocks (Nesbitt and Young 1982). The degree of weathering on sedimentary rocks can be determined by the chemical index of alteration (CIA) proposed by Nesbitt and Young (1982), using molecular proportions:

$$\text{CIA} = [\text{Al}_2\text{O}_3 / (\text{Al}_2\text{O}_3 + \text{CaO}^* + \text{Na}_2\text{O} + \text{K}_2\text{O})] \times 100,$$

where CaO^* is the amount of CaO incorporated in the silicate fraction of the rocks. The degree of weathering increases with increasing CIA, although uncertainties exist in interpreting the CIA due to mobility of alkali and alkaline earth elements. The CIA values determined for the Permo-Carboniferous black shales and sandstones of the Spiti area, Tethys Himalaya (CIA 54–78) (Javid et al. 2014) suggest that the source rocks underwent low-to-moderate weathering during deposition.

4.3 Provenance of the sedimentary rocks

Sedimentary provenance studies have focused on the use and limitations of REEs as provenance indicators for more than 30 years (McLennan et al. 1993; Cullers 2000; Condé et al. 2001; Singh and Rajamani 2001; Lawrence and Kamber 2006). Although REE mobilization can occur during chemical weathering of bedrock, source bedrock REE signatures are preserved in the weathering profile because there is no net loss of REE abundance (Condé

Table 2 Trace elements including REE concentration (ppm) of siliciclastic sedimentary rocks from Spiti region, Tethys Himalaya, India

Element	MLP-1	MLP-3	LSP-1	LSP-3	LSP-6	LSP-7	LSP-9	GLN-1	GLN-3	GLN-5	GLN-6	GLN-9
Sandstones												
La	29.718	8.905	4.088	26.208	9.46	16.076	23.595	13.825	10.584	44.948	15.884	36.658
Ce	57.479	15.99	7.614	51.426	20.754	31.846	51.46	18.932	22.097	89.234	32.913	78.036
Pr	7.018	1.896	0.861	6.044	2.706	3.704	5.157	3.6	2.823	10.233	3.842	7.54
Nd	26.138	6.517	2.871	21.622	10.732	13.44	19.654	13.58	10.982	37.112	14.138	28.128
Sm	5.155	1.147	0.45	3.996	2.435	2.726	3.882	2.581	2.587	6.961	2.736	5.187
Eu	1.294	0.168	0.049	0.736	0.528	0.564	0.699	0.437	0.456	1.366	0.493	0.899
Gd	4.653	1.079	0.369	3.751	2.311	2.625	3.213	2.275	2.261	6.455	2.231	4.312
Tb	0.767	0.213	0.06	0.658	0.464	0.472	0.46	0.386	0.388	1.127	0.358	0.596
Dy	3.962	1.277	0.281	3.448	2.692	2.537	2.44	1.952	1.911	5.982	1.796	3.143
Ho	0.72	0.266	0.058	0.65	0.483	0.49	0.51	0.375	0.322	1.164	0.331	0.66
Er	1.93	0.728	0.158	1.849	1.259	1.303	1.29	1.055	0.834	3.277	0.931	1.671
Tm	0.31	0.125	0.027	0.318	0.195	0.207	0.202	0.186	0.123	0.541	0.152	0.255
Yb	1.821	0.736	0.161	1.836	1.196	1.181	1.117	1.07	0.723	3.278	0.949	1.362
Lu	0.284	0.118	0.027	0.286	0.182	0.2	0.164	0.181	0.112	0.522	0.163	0.204
Th	12.468	6.906	1.311	10.477	3.295	5.057	8.844	5.159	3.664	17.951	5.079	15.991
U	0.023	0.001	0.007	0.013	0.003	0.004	0.015	0.123	0.025	0.036	0.042	0.013
$\sum \text{REE}$												
	141.24	39.16	17.074	122.8	55.397	77.3	113.8	60.435	56.203	212.2	76.917	168.6
Eu/Eu*	0.8074	0.46	0.367	0.58	0.68	0.644	0.6048	0.551	0.576	0.627	0.609	0.58
Ce/Ce*	0.932	0.9117	0.950	0.957	0.961	0.9669	1.0930	0.62877	0.947	0.974	0.987	1.099
(Gd/Yb) _N	2.070	1.188	1.857	1.655	1.566	1.801	2.3312	1.7231	2.5345	1.59	1.905	2.565
La/Yb	16.319	12.09	25.391	14.27	7.909	13.612	21.123	12.920	14.639	13.71	16.73	26.91
(La/Yb) _N	11.027	8.176	17.158	9.646	5.344	9.1984	14.2742	8.73106	9.8922	9.2658	11.31	18.187
La/Th	2.383	1.2894	3.118	2.501	2.871	3.1789	2.66791	2.679	2.888	2.503	3.127	2.292
Th/Yb	6.846	9.383	8.1428	5.70	2.755	4.28196	7.91763	4.82149	5.0677	5.47	5.351	11.74
(La/Sm) _N	3.628	4.8867	5.7180	4.128	2.445	3.7119	3.825	3.3714	2.57513	4.064	3.654	4.44
Element	MLP-6	MLP-8	BS-1	BS-4	BS-5	BS-6	BS-8	TBP-3	TBP-2	TBP-8	TBP-11	TBP-13
Black shales												
La	51.976	33.948	32.42	24.714	29.067	34.434	36.103	54.914	46.362	54.654	50.506	43.187
Ce	118.53	78.334	90.227	108.202	133.873	144.436	157.344	119.634	103.511	141.034	128.581	109.011
Pr	11.18	7.754	9.159	6.419	8.181	8.915	9.813	11.910	10.132	12.024	10.608	8.955
Nd	37.796	28.27	36.705	25.11	32.3	34.272	37.784	48.257	37.648	44.238	38.842	32.236
Sm	5.373	5.122	7.534	5.233	6.453	6.808	7.198	11.406	7.212	8.100	7.018	5.988
Eu	0.762	0.912	1.341	0.928	1.181	1.224	1.304	1.757	1.194	1.444	1.164	0.985
Gd	4.351	4.622	6.193	4.342	5.278	5.073	5.523	10.106	5.958	6.404	5.759	5.516

Table 2 continued

Element	MLP-6	MLP-8	BS-1	BS-4	BS-5	BS-6	BS-8	TBP-3	TBP-2	TBP-8	TBP-9	TBP-11	TBP-13	GLN-2	GLN-4	GLN-7	GLN-8	
Tb	0.574	0.755	0.953	0.681	0.832	0.821	0.802	1.402	0.751	0.771	0.697	0.630	0.631	0.912	0.58	1.027	1.096	
Dy	3.169	4.604	5.166	3.843	4.673	4.656	4.298	6.959	3.871	3.944	3.326	3.131	3.357	4.682	3.18	5.395	5.689	
Ho	0.709	1.052	1.071	0.846	0.988	0.994	0.943	1.243	0.776	0.795	0.651	0.601	0.691	0.976	0.6	1.13	1.193	
Er	2.082	2.732	2.602	2.073	0.539	2.494	2.396	2.698	1.940	2.029	1.621	1.503	1.745	2.546	1.6	2.926	3.01	
Tm	0.36	0.442	0.394	0.334	0.411	0.408	0.387	0.382	0.294	0.315	0.230	0.216	0.269	0.394	0.26	0.435	0.462	
Yb	2.042	2.376	2.106	1.792	2.153	2.116	2.135	1.935	1.588	1.697	1.209	1.169	1.462	2.098	1.424	2.313	2.564	
Lu	0.31	0.343	0.293	0.266	0.324	0.315	0.287	0.268	0.236	0.246	0.179	0.162	0.227	0.318	0.207	0.349	0.362	
Th	23.861	16.631	16.836	14.474	16.653	17.156	19.63	17.348	19.671	21.193	21.329	19.584	15.874	21.687	9.127	24.697	28.625	
U	0.031	0.022	0.028	0.08	0.078	0.104	0.104	1.162	1.092	2.233	4.193	1.706	1.434	3.676	0.023	0.012	0.005	0.011
ΣREE	239.2	171.2	196.1	184.78	226.2	246.9	266.3	272.8	221.5	277.6	250.3	213.2	171.66	199.79	116.73	255.5	281.57	
Eu/Eu*	0.481	0.57	0.599	0.5949	0.618	0.636	0.63	0.5	0.55	0.61	0.55	0.52	0.53	0.57	0.514	0.569	0.57	
Ce/Ce*	1.152	1.131	1.226	2.0128	2.034	1.931	1.958	1.09	1.119	1.289	1.30	1.298	1.134	1.142	1.12	1.142	1.104	
(Gd/Yb) _N	1.726	1.576	2.383	1.963	1.986	1.9430	2.09	4.23	3.04	3.05	3.86	3.8	2.655	2.48	2.25	2.55	2.40	
La/Yb	25.45	14.28	15.3	13.79	13.50	16.273	16.9	28.37	29.19	32.2	41.7	36.94	24.54	17.15	14.36	21.62	23.21	
(La/Yb) _N	17.20	9.655	10.40	9.31	9.123	10.996	11.43	19.17	19.7	21.76	28.2	24.96	16.58	11.59	9.708	14.61	15.68	
La/Th	2.178	2.0412	1.92	1.707	1.745	2.007	1.839	3.16	2.35	2.57	2.36	2.20	2.26	1.65	2.24	2.025	2.079	
Th/Yb	11.68	6.999	7.994	8.077	7.7347	8.107	9.194	8.96	12.4	12.49	17.64	16.75	10.85	10.33	6.409	10.67	11.16	
(La/Sm) _N	6.0	4.171	2.708	2.97	2.83	3.183	3.157	3.03	4.04	4.24	4.53	4.539	4.15	2.91	2.71	3.60	4.20747	

Eu/Eu* = Eu_N/(Sm_N × Gd_N)^{1/2}, Ce/Ce* = Ce_N/(La_N × Pr_N)^{1/2}. N = Chondrite-normalised values (after Sun and McDonough 1989)

et al. 1991; Cullers 2000; Compton et al. 2003; Küllerolf et al. 2008). Because of this, REE ratios [e.g. $(La/Yb)_N$, $(Gd/Yb)_N$, $(La/Sm)_N$, Eu/Eu^*] of sediments are considered to resemble provenance and are commonly used to determine bulk source composition (Singh and Rajamani 2001; Küllerolf et al. 2008; Garzanti et al. 2010; Dabard and Loi 2012). However, large variation among the Permo-Carboniferous sedimentary rocks of the Spiti Region reveals that, despite having the same source, REE concentration can fluctuate during sediment production and transport. In addition to mineralogical control, REE concentrations during sediment production and transport largely depend on processes that operate during sediment deposition such as hydraulic sorting and the quartz dilution effect. Because hydraulic sorting affects minerals that host most of the REEs (e.g. zircon, monazite, allanite, titanite, apatite, xenotime, garnet, etc.), the concentration of these minerals, particularly ultradense minerals, varies with the intensity of hydrodynamic processes (Garzanti et al. 2010).

The emplacement of huge volumes of Proterozoic granites along a length of nearly 2,000 km is considered an important episode of acidic magmatism in the history of crustal growth in the Himalaya and is said to mark the Archean-Proterozoic boundary (Sharma and Rashid 2001). Proterozoic granites of the Himalaya are confined to a linear belt (Fig. 4) and are associated with the same tectono-magmatic event as, but are older than, surrounding volcano-sedimentary sequences. The average REE pattern of the Permo-Carboniferous siliciclastic sedimentary rocks from the Spiti area, Tethys Himalaya matches well with the average REE patterns of Proterozoic granites (Fig. 5) such as the Bandar Gneiss, Wangtu Gneiss/Granites, and Bomdila Gneiss. Proterozoic granites may have played a crucial role in the crustal evolution of the Himalaya. The uplift, unroofing, and erosion of these granites may have supplied ample detritus to the nearby Tethyan sedimentary basin and significantly contributed to the changing of crustal composition of the Himalaya towards a more felsic composition during the post-Archean.

From the above discussion, it is understood that the post-Archean Himalayan REE patterns and Th data indicate the most evolved felsic composition of the source rocks. There are two possibilities for the felsic nature of the post-Archean crust. First, the intrusion of K-rich granites at the end of Archean times is widely accepted. We do not have any evidence for a granitic intrusion in the Himalaya older than 1,900 Ma (Sharma and Rashid 2001). However, some earlier work, based on paleocurrent studies, proposed that the source rocks for these sediments might have been the Aravalli-Delhi mountain chain and Bundelkhan massif (Valdiya 1995). Na-rich (oldest) and K-rich (youngest) phases (Mondal and Zainuddin 1997) of the Bundelkhan massif in the Archean period (3.3 Ga) might be the source

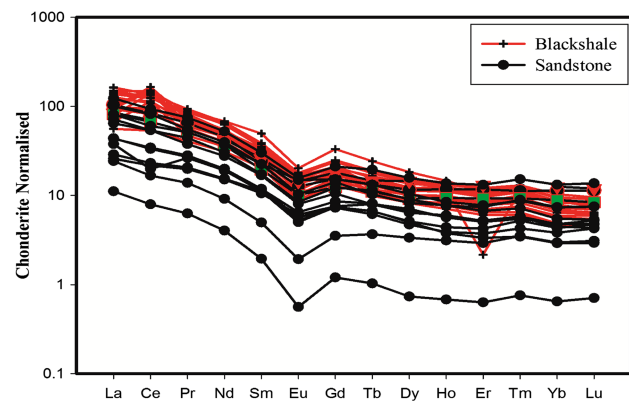


Fig. 2 Chondrite-normalized REE patterns of the Permo-Carboniferous Spiti sedimentary rocks and average chondrite values are from Sun and McDonough (1989)

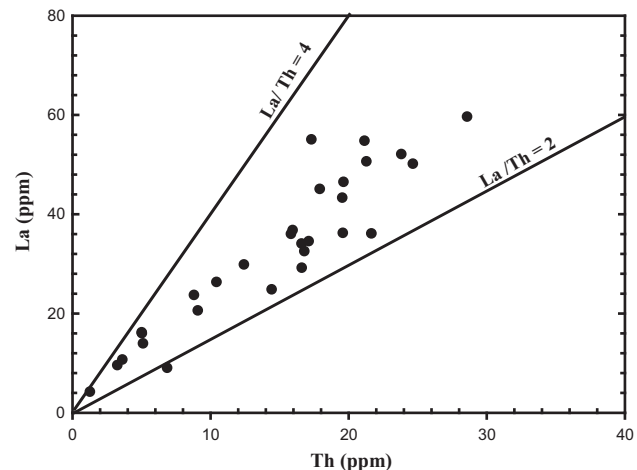


Fig. 3 La vs Th diagram (after McLennan et al. 1980) for the Spiti sedimentary rocks. The Spiti sample La/Th ratios fall in between 2 and 4

of felsic post-Archean Himalayan sediments. A similar conclusion was made by Naqvi and Hussain (1972), following extensive studies from the southern Indian shield where they observed a change in the composition of the upper crust from mafic to felsic during the Archean-Proterozoic because of the emplacement of acid (sodic) plutons into the early Archean crust. Moreover, a good comparison between the REE patterns of the Permo-Carboniferous siliciclastic sedimentary sequences from the NW Tethys Himalaya and the REE patterns of the granitoids from the Himalaya (Fig. 5) further confirm the felsic composition of the source rock. The second possibility to explain the felsic nature of the post-Archean crust is rooted in the sedimentary environment, i.e. oxidizing conditions prevailing during post-Archean times. Based on REE studies of the early Proterozoic sediments, several geoscientists have convincingly argued that the REE patterns

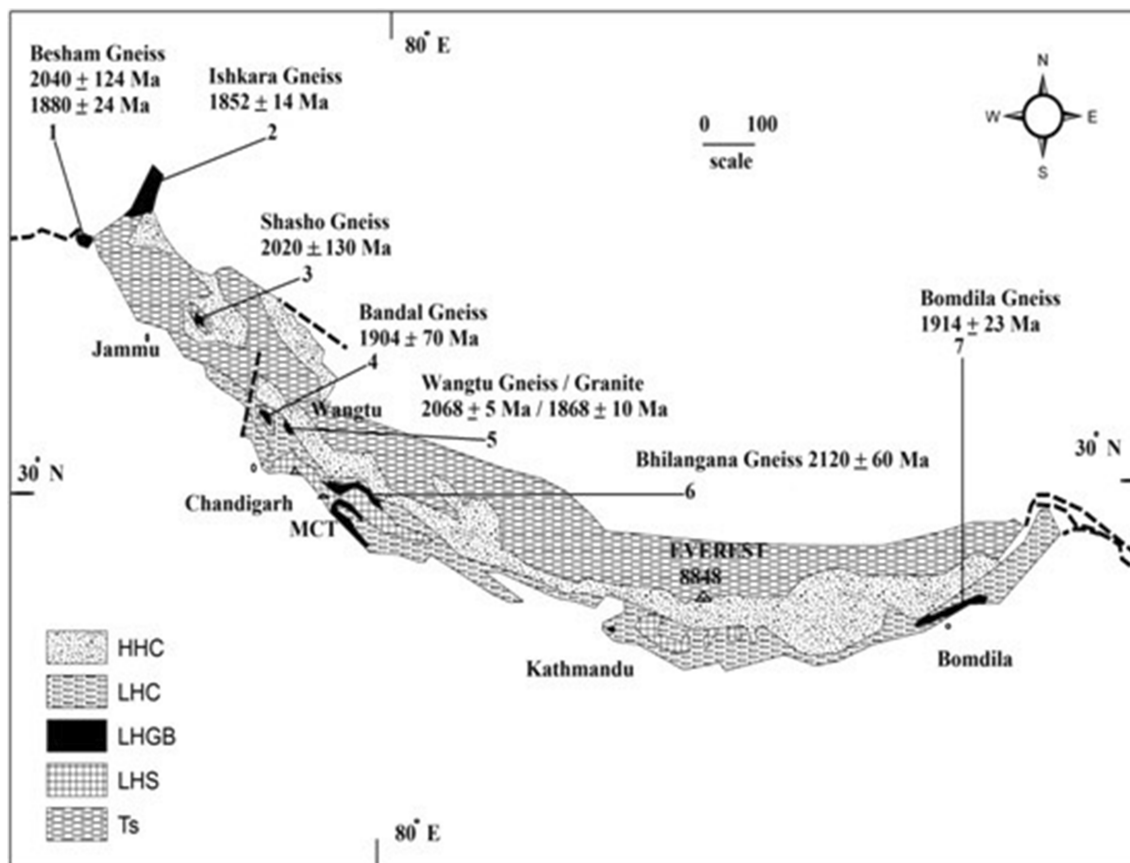


Fig. 4 Geological map (after Sharma 1983) showing the occurrences of Paleoproterozoic granitoids along the lesser Himalaya. Sources of age data: 1—Treloar and Rex 1990; 2—Zeitler et al. 1989; 3—Bhanot et al. 1988; 4—Frank et al. 1977; 5—Singh et al. 1993; 6—Raju et al. 1982; Trivedi et al. 1984; 7—Dikshitulu et al. 1995; Rao 1998

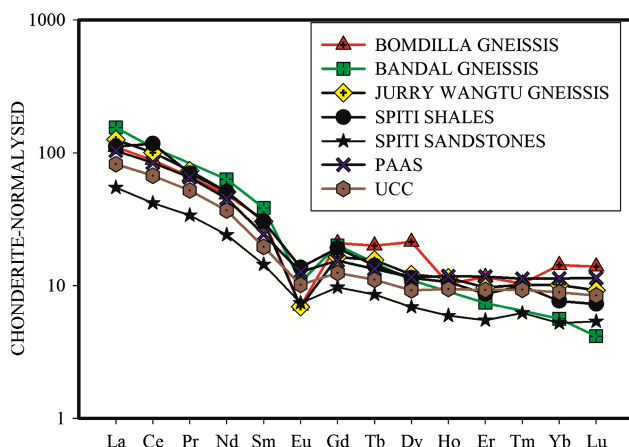


Fig. 5 Average REE pattern of the Permo-Carboniferous siliciclastic sedimentary rocks from the Spiti area, Tethys Himalaya, and Proterozoic granites such as Bandal Gneiss, Wangtu Gneiss/Granites, and Bomdilla Gneiss

(including Eu anomalies), though mostly dependent on their provenance, can also be controlled by fO_2 and sedimentary environment. They observed that when fO_2 is

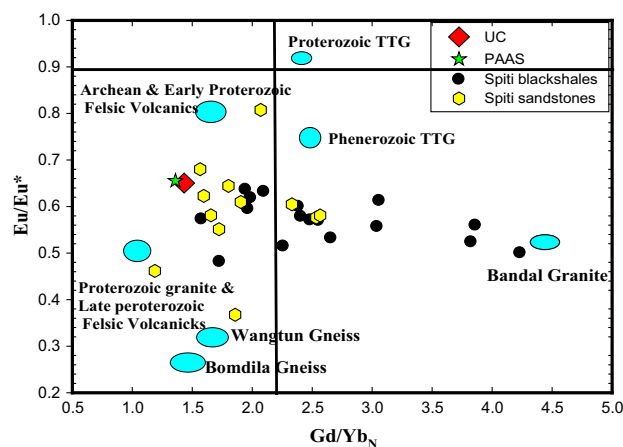


Fig. 6 $(Gd/Yb)_N$ vs. Eu/Eu^* diagram of the Spiti Sedimentary rocks compared with Paleoproterozoic Himalayan Granitoids/Gneisses

low (a reducing environment), the sediments deposited should be characterized by low $\sum\text{REE}$ values and a positive Eu anomaly, whereas sediments deposited in oxidizing conditions (i.e., fO_2 is high) should be characterized by high $\sum\text{REE}$ and Eu depletion. From this

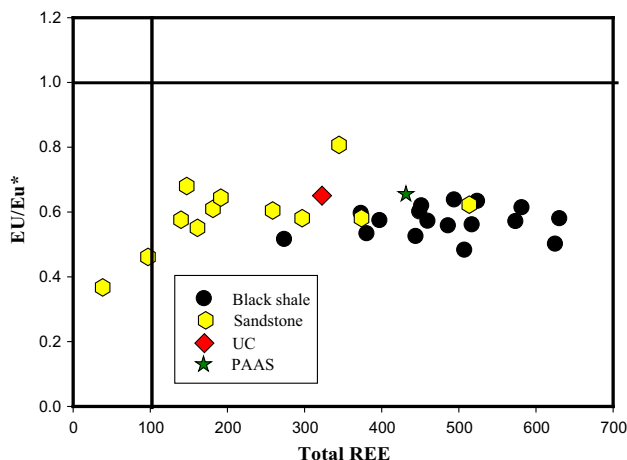


Fig. 7 Plot of Eu/Eu* vs total REE of Permo-Carboniferous siliciclastic sediments from the Spiti Region, Tethys Himalaya

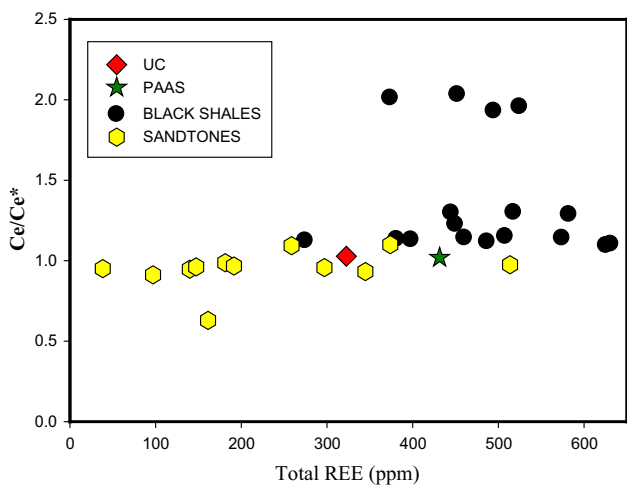


Fig. 8 Plot of Ce/Ce* vs total REE of Permo-Carboniferous siliciclastic sediments from the Spiti Region, Tethys Himalaya

discussion regarding the reduction (Early Archean)—oxidation (post-Archean) mechanism, it appears that the post-Archean clastic sedimentary rocks of NW Tethys Himalaya which are characterized by high \sum REE and a strong negative Eu anomaly were deposited in an oxidizing environment.

4.4 Significance of Eu and Ce anomalies

Understanding the origin of Eu depletion relative to the other chondrite-normalized REEs in clastic sedimentary rocks is fundamental to any interpretation of crustal composition and evolution. The most significant observation in this regard is that virtually all post-Archean sedimentary rocks (sandstones, mudstones, and carbonates) are characterized by Eu depletion of comparable magnitude (Taylor and McLennan 1988). That Eu anomalies seen in post-

Archean sedimentary rocks are due to oxidation-reduction processes during weathering or the breakdown of feldspars is unfounded since there is no significant upper crustal reservoir with the complementary Eu enrichment. The only tenable explanation is that the Eu depletion in sedimentary rocks, and hence the UCC, is due to chemical fractionation within the continental crust, related to production of K-rich granitic rocks which typically possess negative Eu anomalies. The presence of a Eu anomaly is thus the signature of earlier events in a more reducing igneous environment than now exists in the upper crust. Eu/Eu* is typically ≥ 1.0 for Archean sediments and 0.6–0.7 for post-Archean shales (McLennan et al. 1990). Archean sedimentary rocks generally show HREE depletion resulting in high Gd_N/Yb_N ratios, commonly greater than 2.0; whereas Gd_N/Yb_N for post-Archean rocks they is typically 1.0–2.0 (McLennan 1989). However, this ratio can be sensitive to heavy mineral accumulation. For example, McLennan (1989) noted that even small amounts of zircon within a sediment can lead to Gd_N/Yb_N < 1, while the presence of only 0.005 % monazite will increase the Gd_N/Yb_N to > 2. The REE characteristics of the sedimentary rocks from the study area are summarized in Fig. 6 where Eu/Eu* is plotted against Gd_N/Yb_N. There is a spread of average values of Gd_N/Yb_N and Eu/Eu* for Paleo-Proterozoic Himalayan Granitic bodies occurring south of the Spiti basin. These include the Bandal Gneiss, Wangtu Gneiss/Granites, and Bomdila Gneiss—all potential source rocks that could have provided sediment to the basins under discussion—indicating that the Permo-Carboniferous sediments may have received inputs from all of the Proterozoic Himalayan Granitic belt (Fig. 6).

Customarily, sediment Eu/Eu* values are thought to be inherited directly from the source rock (Taylor and McLennan 1985; Borges et al. 2008; Singh 2010). Spiti sediments have Eu/Eu* values ranging from 0.8 to as low as 0.48 with an average 0.57 (Table 1). The covariation between negative Eu anomalies, a decrease in grain size, and an increase in total REE (Fig. 7) suggest the Eu anomaly could be controlled by the accessory phases in the Permo-Carboniferous sandstones and shale sediments. If the negative Eu anomalies are the result of accessory mineral concentration, the Permo-Carboniferous sediments indicate that hydraulic sorting, even over short transport distances, is capable of concentrating enough accessory phases to influence REE composition and to develop negative Eu anomalies that are typically interpreted to represent more felsic, granitic rocks.

The use of the Ce anomaly was first proposed by Elderfield and Greaves (1982) as a consequence of the change in the ionic state of Ce as a function of oxidation state. Ce has two redox states, III and IV. Unlike other lanthanide elements, which are trivalent (except Eu which can be

divalent), Ce³⁺ can be oxidized to Ce⁴⁺ under oxidizing conditions. Ce(IV) is insoluble and, under oxidizing conditions, is precipitated as CeO₂. Thus, sediments deposited under oxic or anoxic conditions can preserve the geochemical signature of Ce³⁺ or Ce⁴⁺, though this signature can be altered, post-depositionally, by late diagenesis and metamorphism. Oxidation of Ce commonly leads to fractionation of Ce from the other REEs. This fractionation generally occurs within pore waters during diagenesis, where REE³⁺ are mobilized from Fe and Mn oxyhydroxides and other unstable REE carriers, leaving Ce⁴⁺ behind. A change in Ce/Ce* during diagenesis has been documented by German and Elderfield (1990) and Murray et al. (1991). Moreover, changes in the oxygen content of marine systems and a heterogeneous source of REE to sediments have also been shown to affect Ce/Ce* (MacLeod and Irving 1996; Murray et al. 1990, 1991; Wright et al. 1987). Normal seawater contains anomalously low concentrations of Ce because it is the only REE that can easily be oxidized to its relatively insoluble 4⁺ valence state under normal surface conditions. Marine authigenic precipitates (carbonates, phosphates, and cherts) may retain this seawater Ce anomaly, in which case oxic bottom waters are indicated (Holser 1997; Shields and Stille 2001). Positive Ce anomalies indicate anoxia in the water column, enhancing Ce(III) concentrations in the sediment (Kato et al. 2002; Sholkovitz et al. 1992). Negative Ce anomalies suggest suboxic conditions wherein aqueous Ce(III) is depleted (Kakuwa and Matsumoto 2006). It is premature to assign quantitative meaning to the absolute values of measured Ce in the whole rock. That is, as yet, a scalar relationship between the Ce anomaly and Eh or the fugacity of oxygen, and, secondarily, a direct relationship between depth of water and the absolute value of the Ce anomaly, is still to be defined. However, for uniform depositional and source conditions, it should be possible to interpret relative change with a range from anoxic (negative) to oxic (positive) values. Murray et al. (1990, 1991) have shown that the Ce anomaly depends on depositional setting. Thus, increasing values indicate more oxic conditions, whereas decreasing values indicate more reducing or anoxic conditions. The removal of dissolved Ce³⁺ as an insoluble form of Ce⁴⁺ preferentially occurs in the upper part of the water column, so oxic seawater shows a negative Ce anomaly, whereas oxic sediments have a less negative to a positive value (Wright et al. 1987). Conversely, in anoxic sediments, Ce is released and the sediments show a negative anomaly. Most of the black shales, Cambrian chert-phosphorite assemblages, and fossil apatite discussed during past years have a positive Ce anomaly associated with anoxic sediments during warmer climate and transgressive conditions (Wright et al. 1987; Wilde et al. 1996; Mazumdar et al. 1999). In other words, the observed Ce anomaly is not limited to

marine carbonate, conodonts, and ichthyoliths, while the whole-rock Ce anomaly can be used as an indicator of intensity of anoxia and therefore of eustatic sea level. A positive-trending whole-rock cerium anomaly indicates more oxic conditions or a sea-level fall. In contrast, a negative-trending anomaly indicates more reducing conditions or a sea-level rise (Wilde et al. 1996).

Another possible cause of Ce anomalies is Ce fractionation at some stage in the weathering and sedimentary processes. In the early stages, negative Ce anomalies are noticed in weathering products like secondary hydrous phosphates (Braun et al. 1990) and positive Ce anomalies emerge in deeply weathered and lateritic profiles where soluble Ce³⁺ oxidizes to insoluble, stable Ce⁴⁺ and is hosted in secondary cerianite, Ce(IV)O₂ (Braun et al. 1990; Borges et al. 2008).

The consistent positive cerium anomalies observed in the Spiti sediments (Fig. 8) are inconsistent with the anoxic depositional environment of these sediments (particularly black shales). In an attempt to explain this anomaly in the Spiti sediments, the following possibilities are proposed. The strong correlation between Ce anomalies, total REE, and grain size (Fig. 6) suggest that the positive anomalies of an anoxic environment may have developed due to post-depositional processes, such as late diagenesis or metamorphism. Moreover, an excellent correlation of La and Ce to Th (0.9) and their high La + Ce contents, suggest that the Th is probably contained chiefly in heavy mineral monazite that may cause enrichment of Ce in the sediments. Since positive Ce anomalies in the sediments have a strong correlation with the sea level eustatic changes (Wilde et al. 1996), a fall in sea level or regressive event at the terminal phase of Carboniferous period in the Spiti area is very well recorded in these sediments.

5 Conclusion

The trace element chemical composition and REE patterns of the Permo-Carboniferous siliciclastic sedimentary rocks of the Kanawar Group, Sipti Region, Tethys Himalaya record compositional changes in provenance. The patterns exhibit LREE enrichment and almost flat HREE trends with large negative Eu anomalies which are typical of post-Archean UCC. The large ion lithophile element, high field strength cation, and REE contents; and La/Th ratios of the siliciclastic sedimentary rocks are consistent with a felsic source rock. Thus, the Permo-Carboniferous siliciclastic sedimentary rocks appear to be derived from sources rich in granitic components, with lesser contributions from basalt, tonalite, and Komatiite. The felsic composition is thought to be related to the emplacement of granitic magma, likely Proterozoic granites of the Himalaya that are confined to a

linear belt. The granitic magmatism that took place for a period of around 800 Ma might have contributed ample material for the later-formed sedimentary basins including Lesser Himalayan sequences, Higher Himalayan sedimentary sequences, and Tethys Himalayan sedimentary sequences (present study) and may have become the primary cause for compositional change of UCC in the Himalaya from mafic to relatively felsic during the post-Archean period. The REE characteristics and Th/U ratios of these sedimentary rocks seem to be affected by both the provenance of the sediments and the sedimentary environment. The sedimentary REE characteristics and Th/U contents suggest that the atmosphere was oxic in the post-Archean.

Acknowledgments The authors express their thanks to the Chairman, Department of Geology, Aligarh Muslim University, Aligarh, for providing necessary facilities. We are also thankful to the Department of Science & Technology, New Delhi for supporting this research in the form of Research Grant (SR/S4/ES-422/2009) to SAR. Authors are really thankful to the anonymous reviewers who have reviewed the manuscript and given positive and useful comments.

References

- Bagati TN (1990) Lithostratigraphy and facies variation in the Spiti Basin (Tethys) Himachal Pradesh India. *Himalayan Geol* 1:35–47
- Balaram V, Gnaneshwar Rao T (2003) Rapid determination of REEs and other trace elements in geological samples by microwave acid digestion and ICP-MS. *At Spectrosc* 24:206–212
- Barth MG, McDonough WF, Rudnick RL (2000) Tracking the budget of Nb and Ta in the continental crust. *Chem Geol* 165:197–213
- Bhanot VB, Kwatra SK, Kansal AK (1988) Rb-Sr geochronological studies of granitic rocks of Galhar-Shasho area, Kishtwar region, Kashmir Himalaya, India. Fourth National Symposium on Mass Spectrometry, Indian Institute of Sciences, Bangalore. *Earth Planet Sci* 13:1–4
- Bhargava ON (2008) An updated introduction to the Spiti Geology. *J Palaeontol Soc India* 53:113–129
- Bhargava ON, Bassi UK (1998) Geology of Spiti-Kinnaur Himachal Himalaya. Geological Survey of India Memoir 124:1–210
- Borges JB, Huh Y, Moon S, Noh H (2008) Provenance and weathering control on river bed sediments of the eastern Tibetan Plateau and the Russian Far East. *Chem Geol* 254:52–72
- Boryta M, Condé KC (1990) Geochemistry and origin of the Archaean Beit Bridge complex, Limpopo Belt, South Africa. *J Geol Soc Lond* 147:229–239
- Braun JJ, Pagel M, Muller JP, Bilong P, Michard A, Guillet B (1990) Cerium anomalies in lateritic profiles. *Geochim Cosmochim Acta* 51:597–605
- Compton JS, White RA, Smith M (2003) Rare earth element behavior in soils and salt pan sediments of a semiarid granitic terrain in the Western Cape, South Africa. *Chem Geol* 20:239–255
- Condé KC (1993) Chemical composition and evolution of the upper continental crust: contrasting results from surface samples and shales. *Chem Geol* 104:1–37
- Condé KC, Wilks M, Rosen DM, Zlobin VL (1991) Geochemistry of metasediments from the Precambrian Hapschan series, eastern Anabar Shield, Siberia. *Precambrian Res* 50:37–47
- Condé KC, Marais DJD, Abbott D (2001) Precambrian superplumes and supercontinents: a record in black shales, carbon isotopes, and paleoclimates. *Precambr Res* 106:239–260
- Cullers RL (1994) The controls on the major and trace element variation of shales, siltstones and sandstones of Pennsylvanian-Permian age from uplifted continental blocks in Colorado to platform sediment in Kansas, USA. *Geochim Cosmochim Acta* 58:4955–4972
- Cullers RL (2000) The geochemistry of shales siltstones and sandstones of Pennsylvanian Permian age, Colorado, USA: implications for provenance and metamorphic studies. *Lithos* 51:181–203
- Dabard MP, Loi A (2012) Environmental control on concretion-forming processes: examples from Paleozoic terrigenous sediments of the North Gondwana margin, Armorican Massif (Middle Ordovician and Middle Devonian) and SW Sardinia (Late Ordovician). *Sed Geol* 267:93–103
- Dikshitulu GD, Pandey BK, Krishna V, Dhana Raju R (1995) Rb-Sr systematics on granitoids of the Central Gneissic Complex, Arunachal Himalaya: implications on tectonic, stratigraphy and source. *J Geol Soc India* 45:51–60
- Draganits E, Mawson R, Talent JA, Krystyn L (2002) Lithostratigraphy conodontbiostratigraphy and depositional environment of the Middle Devonian Givetian to Early Carboniferous Tournaise Lipak Formation in the Pin Valley of Spiti, NW India. *Riv Ital Paleont Stratigr* 108:7–35
- Elderfield H, Greaves MJ (1982) The rare earth elements in seawater. *Nature* 296:214–219
- Frank W, Thoni M, Purtscheller F (1977) Geology and petrology of Kulu-South Lahul area. In: Himalayas, vol 268. *Science de la Terre*, C.N.R.S., Paris, pp 142–172
- Gaetani M, Garzanti E (1991) Multicycle history of the northern India continental margin northwestern Himalaya. *Am Assoc Pet Geol Bull* 75:1427–1446
- Garzanti E, Angiolini L, Sciunnach D (1996) The mid-Carboniferous to lowermost Permian succession of Spiti Po Group and Ganmachidam formation Tethys Himalaya, northern India: Gondwana glaciation and rifting of Neo-Tethys. *Geodin Acta* 9:78–100
- Garzanti E, Ando S, France-Lanord C, Vezzoli G, Censi P, Galy V, Najman Y (2010) Mineralogical and chemical variability of fluvial sediments. 1. Bed-load sand: Ganga-Brahmaputra, Bangladesh. *Earth Planet Sci Lett* 299:368–381
- Garzanti E, Ando S, France-Lanord C, Censi P, Vignola P, Galy V, Lupker M (2011) Mineralogical and chemical variability of fluvial sediments 2. Suspended-load silt: Ganga-Brahmaputra, Bangladesh. *Earth Planet Sci Lett* 302:107–120
- German CR, Elderfield H (1990) Rare earth elements in the NW Indian Ocean. *Geochim Cosmochim Acta* 54:1929–1940
- Holser WT (1997) Geochemical events documented in inorganic carbon isotopes. *Palaeogeogr Palaeoclimatol Palaeoecol* 132:173–182
- Javid AG, Rashid SA, Masroor Alam M, Balaram V, Sathynarayanan M (2014) The geochemistry of Permo-Carboniferous black shales from Spiti region, Himachal Pradesh, Tethys Himalaya: a record of Provenance and change in climate. *Himalayan Geol* 35:31–39
- Kakuwa Y, Matsumoto R (2006) Cerium negative anomaly just before the Permian and Triassic boundary event: the upward expansion of anoxia in the water column. *Palaeogeogr Palaeoclimatol Palaeoecol* 229:335–344
- Kato Y, Nakao K, Isozaki Y (2002) Geochemistry of Late Permian to Early Triassic pelagic cherts from southwest Japan: implications for an oceanic redox change. *Chem Geol* 182:15–34
- Kütterolf S, Diener R, Schacht U, Krawinkel H (2008) Provenance of the Carboniferous Hochwipfel Formation (Karawanken Mountains, Austria/Slovenia) Geochemistry versus petrography. *Sed Geol* 203:246–266
- Lawrence MG, Kamber BS (2006) The behaviour of the rare earth elements during estuarine mixing – revisited. *Mar Chem* 100:147–161

- Liu Y-G, Miah MRU, Schmitt RA (1988) Cerium: a chemical tracer for paleo-oceanic redox conditions. *Geochim Cosmochim Acta* 52:1361–1371
- Macleod KG, Irving AJ (1996) Correlation of cerium anomalies with indicators of paleoenvironment. *J Sediment Res* 66:948–955
- Mazumdar A, Banerjee DM, Schidlowski M, Balaram V (1999) Rare-earth elements and stable isotope geochemistry of early Cambrian chert phosphorite assemblages from the Lower Tal Formation of the Krol Belt, Lesser Himalaya, India. *Chemical Geology* 156:275–297
- McLennan SM (1989) Rare earth elements in sedimentary rocks: influence of provenance and sedimentary processes. *Geochemistry and mineralogy of the rare earth elements*. Rev Mineral Geochim 21:169–200
- McLennan SM (2001) Relationships between the trace element composition of sedimentary rocks and upper continental crust. *Geochim Geophys Geosyst* 2:2000GC000109
- McLennan SM, Taylor SR (1980) Th and U in sedimentary rocks: crustal evolution and sedimentary recycling. *Nature* 285:621–624
- McLennan SM, Taylor SR (1991) Sedimentary rocks and crustal evolution: tectonic setting and secular trends. *J Geol* 99:1–21
- McLennan SM, Nance WB, Taylor SR (1980) Rare earth element–thorium correlations in sedimentary rocks and the composition of the continental crust. *Geochim Cosmochim Acta* 44:1833–1839
- McLennan SM, Taylor SR, McCulloch MT, Maynard JB (1990) Geochemical and Nd–Sr isotopic composition of deep-sea turbidites—crustal evolution and plate tectonic associations. *Geochim Cosmochim Acta* 54:2015–2050
- McLennan SM, Hemming S, McDaniel DK, Hanson GN (1993) Geochemical approaches to sedimentation, provenance, and tectonics. In: Johnson MJ, Basu A (eds) *Processes controlling the composition of clastic sediments*. Geological Society of America Special Paper 284, London, pp 21–40
- McLennan SM, Bock B, Compston W, Hemming SR, McDaniel DK (2001) Detrital zircon geochronology of Taconian and Acadian foreland sedimentary rocks in New England. *J Sediment Res* 71:305–317
- Mondal MEA, Zainuddin SM (1997) Geochemical characteristics of the granites of Bundelkhand massif, central India. *J Geol Soc India Bangalore* 50:69–74
- Moosavirad SM, Janardhana MR, Sethumadhav MS, Moghadam MR, Shankara M (2011) Geochemistry of lower Jurassic shales of the Shemshak Formation, Kerman provenance, Central Iran: Provenance, source weathering and Tectonic setting. *Chem Erde* 71:279–288
- Murray RW, Buchholz Ten Brink MR, Jones DL, Gerlach DC, Price Russ G (1990) Rare earth elements as indicators of different marine depositional environments in chert and shale. *Geology* 18:268–271
- Murray RW, Buchholz Ten Brink MR, Gerlach DC, Russ GP, Jones DL (1991) Rare earth, major, and trace elements in chert from the Franciscan complex and Monterey Group: assessing REE sources to fine grained marine sediments. *Geochim Cosmochim Acta* 55:1875–1895
- Myrow PM, Hughes NC, Paulsen T, Williams I, Parcha SK, Thompson KR, Bowring SA, Peng SC, Ahluwalia AD (2003) Integrated tectonostratigraphic analysis of the Himalaya and implications for its tectonic reconstruction. *Earth Planet Sci Lett* 212:433–441
- Naqvi SM, Hussain SM (1972) Petrochemistry of early Precambrian meta-sediments from the central part of the Chital durg schist belt, Mysore, India. *Chemical Geology* 10:109–135
- Nesbitt HW, Young GM (1982) Early Proterozoic climates and plate motions inferred from major element chemistry of lutites. *Nature* 199:715–717
- Nesbitt HW, Markovics G, Price RC (1980) Chemical processes affecting alkalis and alkali earths during continental weathering. *Geochim Cosmochim Acta* 44:1659–1666
- Raju BNV, Chab Ria T, Prasad RN, Mah Adevan TM, Bhalla NS (1982) Early Proterozoic Rb–Sr isochron age for Central Crystalline, Bhilangana valley, Garhwal Himalaya. *Himal Geol* 12:196–205
- Rao PS (1998) Kameng Orogeny, 1.8–1.9 Ga, from the isotopic evidence of the *Bomdila orthogneisses*, Kameng Sector, NEFA, India. *Geol Bull Univ Peshawar* 31:159–162
- Rashid SA (2005) The Geochemistry of Mesoproterozoic clastic sedimentary rocks from the Rautgara Formation, Kumaun Lesser Himalaya: implications for provenance, mineralogical control and weathering. *Curr Sci* 88:1832–1836
- Sciunnach D, Garzanti E (2012) Subsidence history of the Tethys Himalaya. *Earth Sci Rev* 111:179–198
- Sharma KK (1983) Granitoid belts of the Himalaya. In: Shams FA (ed) *Granites of Himalaya Karakoram and Hindukush*. Institute of Geology, Punjab University, Lahore, pp 11–37
- Sharma KK, Rashid SA (2001) Geochemical evolution of Peraluminous Paleoproterozoic Bandal Orthogneiss, NW Himalaya, Himachal Pradesh, India: implications for the ancient crustal growth in the Himalaya. *J Asian Earth Sci* 19:413–428
- Shields G, Stille P (2001) Diagenetic constraints on the use of cerium anomalies as palaeoseawater redox proxies: isotopic and REE study of Cambrian phosphorites. *Chem Geol* 175:29–48
- Sholkovitz ER, Shaw TJ, Schneider DL (1992) The geochemistry of rare earth elements in the seasonally anoxic water column and pore waters of Chesapeake Bay. *Geochim Cosmochim Acta* 56:3389–3402
- Singh P (2010) Geochemistry and provenance of stream sediments of the Ganga River and its major tributaries in the Himalayan region, India. *Chem Geol* 269:220–236
- Singh P, Rajamani V (2001) REE geochemistry of recent clastic sediments from the Kaveri floodplains, Southern India: implication to source area weathering and sedimentary processes. *Geochim Cosmochim Acta* 65:3093–3108
- Singh S, Sjoberg H, Classon S, Gee D, Jain AK (1993) New U–Pb Proterozoic data from Chor-Wangtu granitoids of Himalayan crystalline belt from Himachal, India. I: Seminar on Himalayan Geology and Geophysics, Abstract Volume Wadia Institute of Himalayan Geology, Dehradun, India, pp 55–56
- Sun SS, McDonough WF (1989) Chemical and isotopic systematics of oceanic basalts: implications for mantle composition and processes. In: Saunders AD, Norry MJ (eds) *Magmatism in the Ocean Basins*. Geological Society of London, Special Publication 42, London, pp 313–334
- Taylor SR, McLennan SM (1985) The continental crust, its composition and evolution. Blackwell, London
- Taylor SR, McLennan SM (1988) The significance of the rare earths in geochemistry and cosmochemistry. In: Gschneider KA Jr, Eyring L (eds) *Handbook on the physics and chemistry of rare Earths*, vol 11. Elsevier, New York, pp 485–578
- Taylor SR, McLennan SM (1995) The geochemical evolution of the continental crust. *Rev Geophys* 33:241–265
- Treloar PJ, Rex DC (1990) Cooling and uplift histories of the crystalline thrust stack of the Indian plate internal zones west of Nanga Parbat, Pakistan Himalaya. *Tectonophysics* 180:323–349
- Trivedi JR, Gopalan K, Valdiya KS (1984) Rb–Sr ages of granitic rocks within the Lesser Himalayan nappes, Kumaun, India. *J Geol Soc India* 25:641–654
- Valdiya KS (1995) Proterozoic sedimentation and Pan African geodynamic development in the Himalaya. *Precambr Res* 74:35–55
- Wilde P, Quinby-Hunt MS, Erdtmann BD (1996) The whole rock cerium anomaly: a potential indicator of eustatic sea-level changes in shales of the anoxic facies. *Sed Geol* 101:43–53
- Wright J, Schrader H, Holser WT (1987) Paleoredox variations in ancient oceans recorded by rare earth elements in fossil apatite. *Geochim Cosmochim Acta* 51:631–644

- Wronkiewicz DJ, Condie KC (1990) Geochemistry and mineralogy of sediments from the Venters dorp and Transvaal Super groups, South Africa: cratonic evolution during the early Proterozoic. *Geochim Cosmochim Acta* 54:343–354
- Yan QR, Geo SL, Wang ZQ, Li JL, Hou QL, Chen HL (2002) Geochemical constraints of the sediments on Provenance, Depositional environment and tectonic Setting of the songliao Prototype basin. *Acta Geol Sinica* 76:445–462
- Zeitler PK, Sutter JF, Williams IS, Zartman R, Tahirkheli RAK (1989) Geochronology and temperature history of the Nanga Parbat-Haramosh massif, Pakistan. In: Malinconico LL, Lillie RJ (eds) Tectonics of the western Himalayas. Geological Society of America Special Paper 232, pp 1–22